

## Electronic Supplementary Information

# Hierarchical porous graphitic carbon for high-performance supercapacitors at high temperature†

Chong Chen,<sup>[a,c]</sup> Dengfeng Yu,<sup>[b]</sup> Gongyuan Zhao,<sup>[a]</sup> Lei Sun,<sup>[a]</sup> Yinyong Sun,<sup>[a]</sup> Kunyue Leng,<sup>[a]</sup> Miao

Yu,<sup>\*[a]</sup> and Ye Sun<sup>\*[b]</sup>

*<sup>a</sup>School of Chemical Engineering and Technology, Harbin Institute of Technology, Harbin 150001,*

*China*

*<sup>b</sup>Condensed Matter Science and Technology Institute, Harbin Institute of Technology, Harbin 150001,*

*China*

\* Corresponding author. E-mail address: miaoyu\_che@hit.edu.cn (M. Yu), sunye@hit.edu.cn (Y. Sun)

## Electrochemical measurement

Carbon product (80 wt%), acetylene black (15 wt%) and polytetrafluoroethylene (PTFE) binder (5 wt%) were mixed in ethanol, then coated onto nickel-foam current collectors ( $1 \times 1 \text{ cm}^2$ ), and dried at  $120 \text{ }^\circ\text{C}$  for 12 h. The mass loading of the active materials in each working electrode was  $\sim 1.5 \text{ mg cm}^{-2}$ . For the three-electrode system, Pt foil and Hg/HgO electrode were used as the counter and reference electrodes, respectively. The electrochemical performance was tested in  $6 \text{ mol L}^{-1}$  KOH electrolyte. For the two-electrode system (2032 stainless steel coin cell, PTFE as insulation), both  $6 \text{ mol L}^{-1}$  KOH and EMIMBF<sub>4</sub> were used as the electrolyte, respectively. The dried electrodes ( $\sim 1.5 \text{ mg cm}^{-2}$ , 0.2 mm in thickness) were symmetrically assembled with glassy paper as the separator in a glove box filled with argon. The cyclic voltammetry (CV), galvanostatic charge-discharge, and electrochemical impedance spectroscopy (EIS) measurements were carried out using an electrochemical workstation (CHI660E, ChenHua Instruments Co. Ltd., Shanghai).

For the three-electrode system, the specific capacitance derived from galvanostatic tests were calculated by the following equations:

$$C_{sp} = \frac{I\Delta t}{m\Delta V} \quad (1)$$

in which  $C$  ( $\text{F g}^{-1}$ ) is the specific capacitance;  $I$  (A) is the discharge current;  $\Delta t$  (s) is the discharge time;  $\Delta V$  (V) is the potential window; and  $m$  (g) is the mass of the active materials.

$$\rho = \frac{1}{V_{total} + \frac{1}{\rho_{carbon}}} \quad (2)$$

in which  $\rho$  ( $\text{g cm}^{-3}$ ) is the density of electrode materials;  $V_{total}$  ( $\text{cm}^3 \text{ g}^{-1}$ ) is the total pore volume of active material measured by nitrogen isotherm; and  $\rho_{carbon}$  is the density of carbon ( $2 \text{ g cm}^{-3}$ ).

$$C_v = C\rho \quad (3)$$

in which  $C_v$  ( $\text{F cm}^{-3}$ ) is the volumetric capacitance;  $C$  ( $\text{F g}^{-1}$ ) is the specific capacitance; and  $\rho$  ( $\text{g cm}^{-3}$ ) is the density of electrode materials.

For the two-electrode system, the specific (or gravimetric) capacitances ( $C$ ,  $\text{F g}^{-1}$ ) were calculated using equation 4 for galvanostatic charge-discharge method and equation 5 for cyclic voltammetry data:

$$C_{sp} = \frac{4I\Delta t}{m\Delta V} \quad (4)$$

$$C = \frac{2}{mv(V_b - V_a)} \int_{V_a}^{V_b} IdV \quad (5)$$

in which  $I$  (A) is the discharge current,  $\Delta t$  (s) is the discharge time,  $\Delta V$  (V) is the potential window,  $v$  ( $\text{V s}^{-1}$ ) is the scan rate,  $V_b$  and  $V_a$  (V) are the high and low potential limit of the CV tests; and  $m$  (g) is the total mass of the active materials.

To construct the Ragone plot, the energy density  $E$  ( $\text{Wh kg}^{-1}$ ) and  $P$  ( $\text{W kg}^{-1}$ ) based on the electrode were calculated by the following equations:

$$E = \frac{1}{8} C_{sp} (\Delta V)^2 \left( \frac{1000}{3600} \right) \quad (6)$$

$$P = 3600 \frac{E}{\Delta t} \quad (7)$$

in which  $C$  ( $\text{F g}^{-1}$ ) is the specific capacitance, and  $\Delta V$  (V) is the potential window, and  $\Delta t$  (s) is the discharge time.

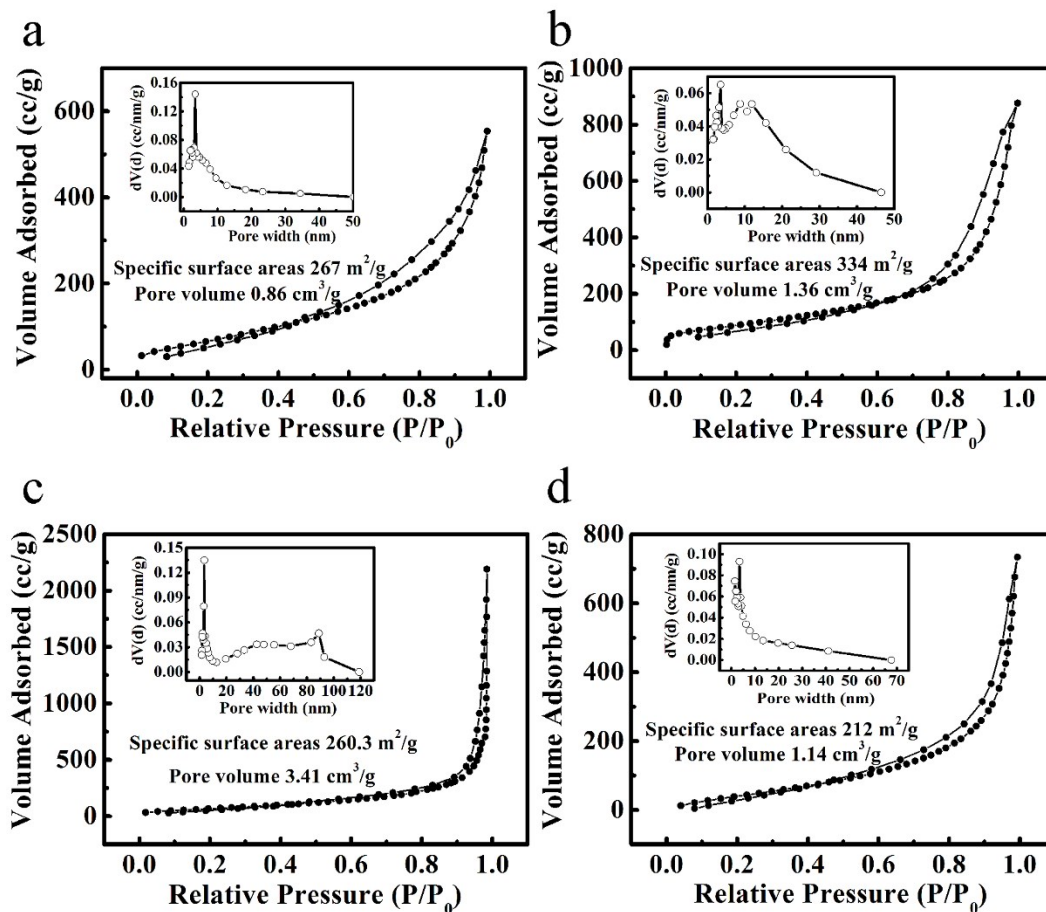


**Fig. S1** The SSA was measured by nitrogen adsorption-desorption isotherms (BeiShiDe Instrument-S&T 3H-2000PS1) after vacuum drying at 120 °C for 1 h. The Brunauer-Emmett-Teller (BET) method was used for calculating the specific surface area, and the Barrett-Joyner-Halenda (BJH) model was used for estimating the pore size distribution. Nitrogen adsorption-desorption isotherm (with the pore size distribution in the inset) of (a) 'GC-Mg/ZA', (b) 'GC-1Mg/U', (c) 'GC-3Mg/U', and (d) 'GC-5Mg/U'.

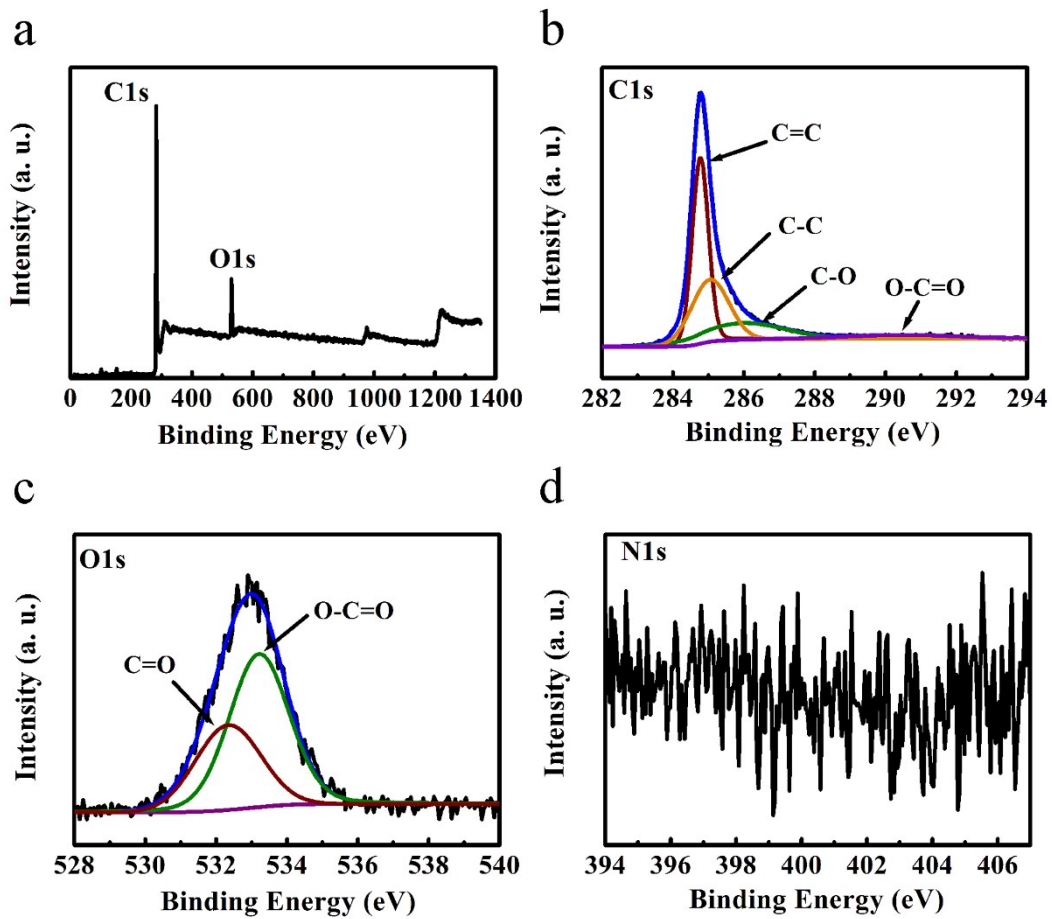
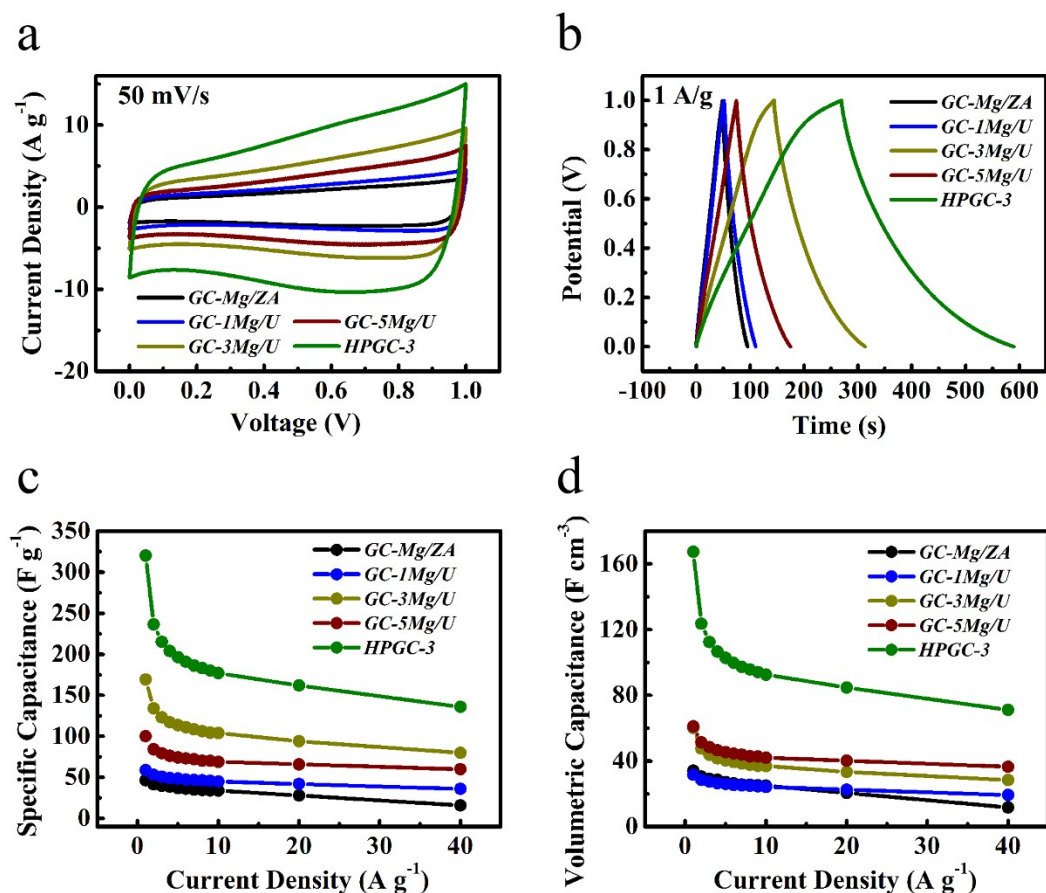


Fig. S2 (a) XPS survey, (b) C1s, (c) O1s and (d) N1s spectra of the 'GC-3Mg/U' sample.



Fig. S3 The urea and zinc acetate dehydrate mixture at the same conditions.



**Fig. S4** Electrochemical performance of all samples measured in a three-electrode system using 6 mol L<sup>-1</sup> KOH electrolyte. (a) CV curves at a scan rate of 50 mV s<sup>-1</sup>. (b) Charge–discharge curves at a current density of 1 A g<sup>-1</sup>. (c) Gravimetric capacitances at different current densities from 1 to 40 A·g<sup>-1</sup>. (d) Volumetric capacitances at different current densities

**Table S1** Comparison of the specific capacitances of previously fabricated hierarchical porous carbons using three-electrode systems.

Materials	Electrolyte	Current Density	Specific Capacitance (F·g <sup>-1</sup> )	Ref. No.
<b>Hierarchical porous graphitic carbon</b>	<b>6 M KOH</b>	<b>1 A·g<sup>-1</sup></b>	<b>320</b>	<b>This work</b>
Hierarchical porous carbon fibers	3 M KOH	1 A·g <sup>-1</sup>	189.7	[1]
Three-dimensional beehive-like hierarchical porous carbons	6 M KOH	1 A·g <sup>-1</sup>	287	[2]
Hierarchical hollow porous carbon spheres	6 M KOH	1 A·g <sup>-1</sup>	303.9	[3]
Hierarchical porous carbons	6 M KOH	0.2 A·g <sup>-1</sup>	283.4	[4]
Porous carbon through hard–soft dual templates	6 M KOH	1 A·g <sup>-1</sup>	153	[5]
Hierarchical porous carbons	6 M KOH	1 A·g <sup>-1</sup>	190	[6]
Nitrogen-doped porous carbon nanofibers	6 M KOH	1 A·g <sup>-1</sup>	202	[7]
Nitrogen and sulfur codoped porous carbon microsphere	6 M KOH	0.1 A·g <sup>-1</sup>	295	[8]
Chlorine-doped ordered mesoporous carbon	6 M KOH	0.5 A·g <sup>-1</sup>	220	[9]

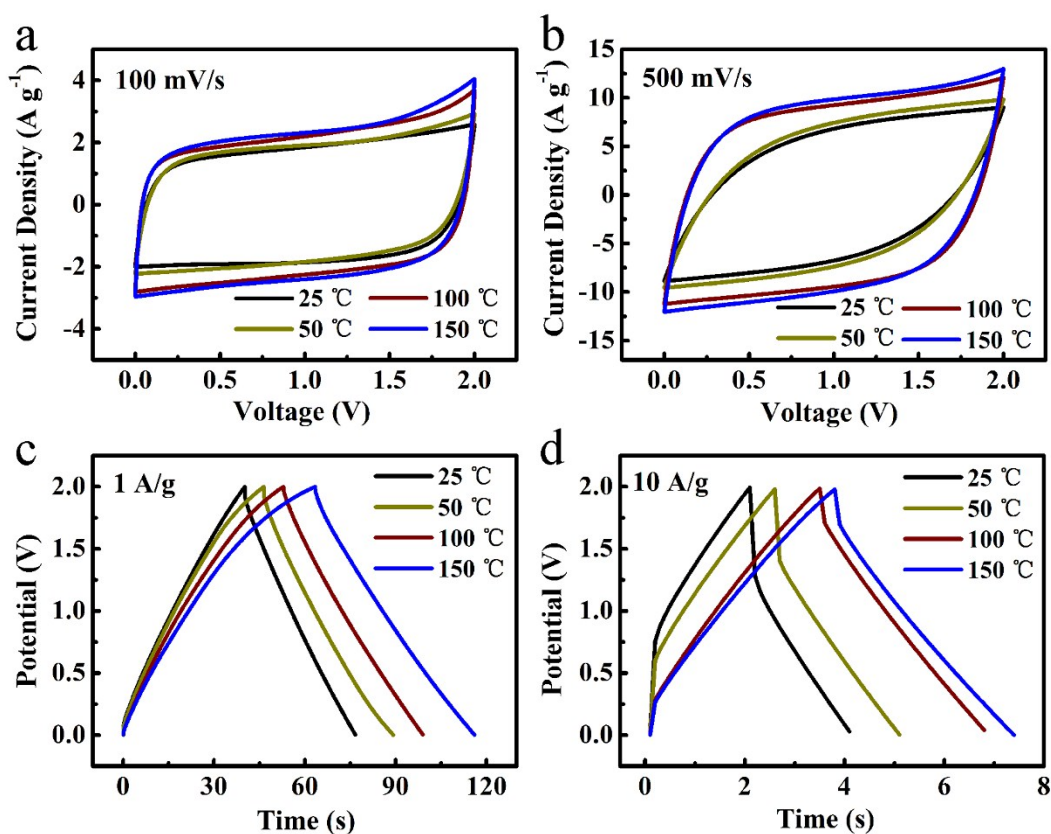


**Fig. S5** Electrochemical performance characteristics of 'HPGC-3' measured in a two-electrode system using EMIMBF<sub>4</sub> electrolyte operating at 25 °C, 50 °C, 100 °C and 150 °C, respectively. CV curves at a scan rate of (a) 100 mV s<sup>-1</sup>; (b) 500 mV s<sup>-1</sup>. Charge-discharge curves at a current density of (c) 1 A g<sup>-1</sup>; (d) 10 A g<sup>-1</sup>.

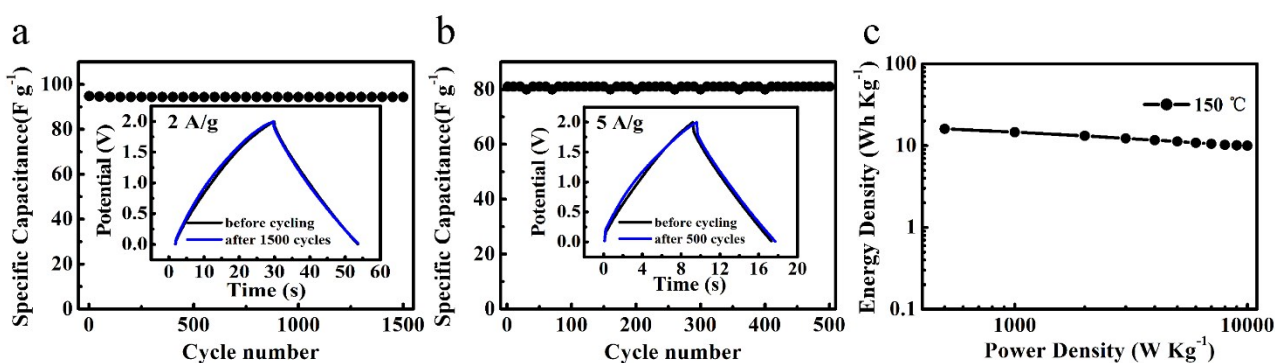


**Fig. S6** (a) Cycling stabilities measured at 2 A g<sup>-1</sup> operating at 150 °C, with the magnified galvanostatic charge-discharge curves before and after 1500 cycles in the inset. (b) Long-term stability of HPGC-3'-based supercapacitors under dynamic thermal stresses, with the magnified galvanostatic charge-discharge curves before and after 500 cycles in the inset. (c) Ragone plot of 'HPGC-3'.

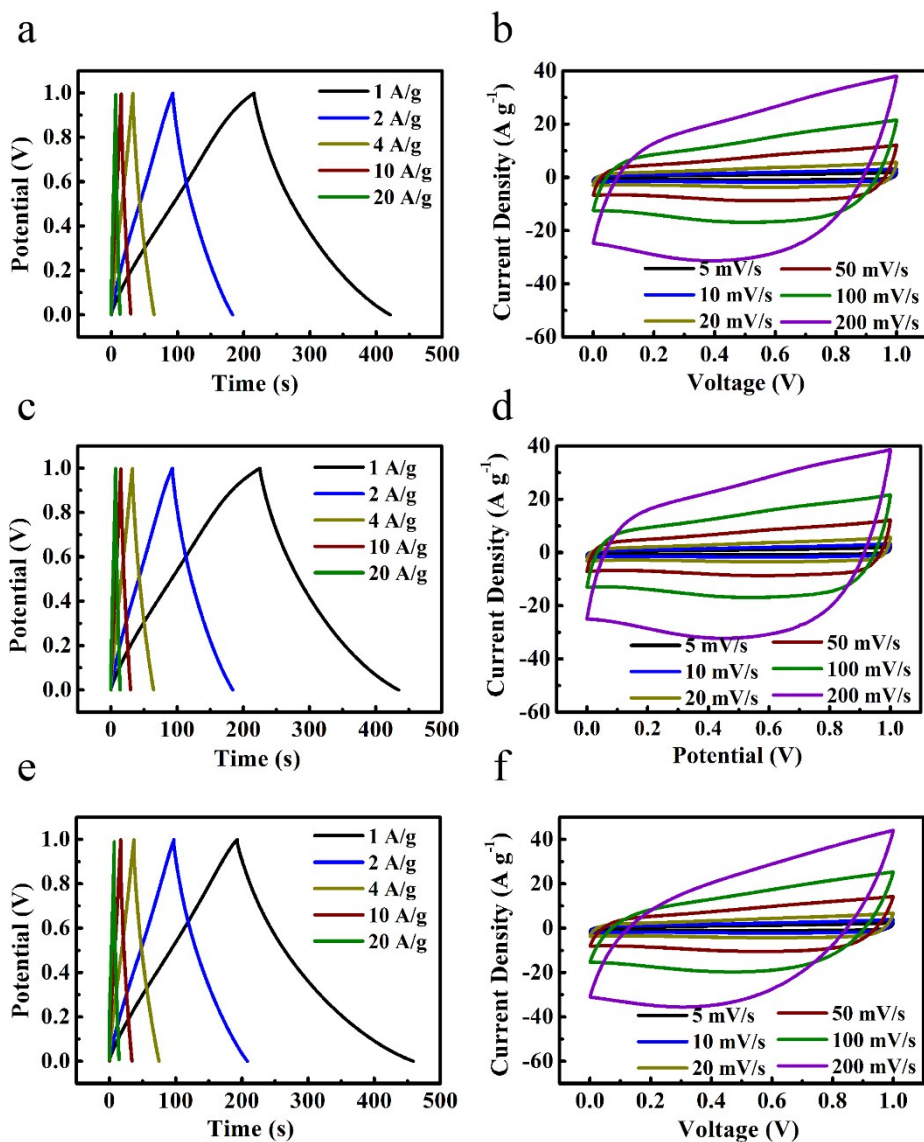


**Fig. S7** Electrochemical performance of ‘*HPGC-3G*’, ‘*HPGC-3P*’ and ‘*HPGC-3H*’ using glycine (G), polyvinylpyrrolidone (P) and hexamethylenetetramine (H) to replace urea during the HPGC synthesis, measured in a three-electrode system in the 6 mol L<sup>-1</sup> KOH electrolyte. Charge–discharge curves of (a) ‘*HPGC-3G*’; (c) ‘*HPGC-3P*’; (e) ‘*HPGC-3H*’ at different current densities. CV curves of (b) ‘*HPGC-3G*’; (d) ‘*HPGC-3P*’; (f) ‘*HPGC-3H*’ at different scan rates.

## References

- [1] Y. Liu, Z. J. Shi, Y. F. Gao, W. D. An, Z. Z. Cao and J. R. Liu, *ACS Appl. Mater. Interfaces*, 2016, **8**, 28283–28290.
- [2] L. Yao, G. Z. Yang, P. Han, Z. H. Tang and J. H. Yang, *J. of Power Sources*, 2016, **315**, 209–217.
- [3] J. Liu, X. Y. Wang, J. Gao, Y. W. Zhang, Q. Lu and M. Liu, *Electrochim. Acta*, 2016, **211**, 183–192.
- [4] S. Wang, T. Wang, P. C. Liu, Y. Shi, G. Liu and J. P. Li, *Mater. Res. Bull.*, 2017, **88**, 62–68.
- [5] X. Y. Chen, C. Chen, Z. J. Zhang and D. H. Xie, *J. Mater. Chem. A*, 2013, **1**, 7379–7383.
- [6] J. B. Zhang, L. J. Jin, J. Cheng and H. Q. Hu, *Carbon*, 2013, **55**, 221–232.
- [7] L. F. Chen, X. D. Zhang, H. W. Liang, M. G. Kong, Q. F. Guan, P. Chen, Z. Y. Wu and S. H. Yu, *ACS NANO*, 2012, **6**, 7092–7102.
- [8] J. C. Zhang, J. S. Zhou, D. Wang, L. Hou and F. M. Gao, *Electrochim. Acta*, 2016, **191**, 933–939.
- [9] Z. K. Kou, B. B. Guo, Y. F. Zhao, S. F. Huang, T. Meng, J. Zhang, W. Q. Li, I. S. Amiin, Z. H. Pu, M. Wang, M. Jiang, X. B. Liu, Y. F. Tang, and S. C. Mu, *ACS Appl. Mater. Interfaces*, 2017, **9**, 3702–3712.